Chin. J. Astron. Astrophys. Vol. 5 (2005), No. 1, 99–109
(*http://www.chjaa.org*)

Chinese Journal of
Astronomy and
Astrophysics

The Influence of Ion-Acoustic Turbulence on the Electron Acceleration in the Reconnecting Current Sheet *

Gui-Ping Wu[1], Guang-Li Huang[2] and Yu-Hua Tang[3]

[1] Department of Physics, Southeast University, Nanjing 210096; *wuguiping@seu.edu.cn*
[2] Purple Mountain Observatory, Chinese Academy of Sciences, Nanjing 210008
[3] Department of Astronomy, Nanjing University, Nanjing 210093

Received 2004 June 26; accepted 2004 November 30

Abstract Through solving the single electron equation of motion and the Fokker-Planck equation including the terms of electric field strength and ion-acoustic turbulence, we study the influence of the ion-acoustic wave on the electron acceleration in turbulent reconnecting current sheets. It is shown that the ion-acoustic turbulence which causes plasma heating rather than particle acceleration should be considered. With typical parameter values, the acceleration time scale is around the order of 10^{-6} s, the accelerated electrons may have approximately a power-law distribution in the energy range $20 \sim 100$ keV and the spectral index is about $3\sim10$, which is basically consistent with the observed hard X-ray spectra in solar flares.

Key words: turbulence – acceleration of particles – Sun: X-rays, gamma rays

1 INTRODUCTION

Particle acceleration in collisionless reconnecting current sheets (hereafter RCS) has been extensively studied (Martens 1988; Martens & Young 1990; Litvinenko 1996, 2003 and references therein), and used to explain observational events (Martens & Kuin 1989; Wu & Xu 1996; Somov et al. 2002). Evidence supporting this model comes from *Yohkoh*/X-ray telescope and SOHO/EIT observations which show that this process indeed occurs above the soft X-ray flare loops and plasmoid eject ed out of the reconnection region (Masuda et al. 1994; Yokoyama et al. 2001). Considering the super electric field acceleration and the small thickness of the predicted collisionless current sheet, current driven instabilities should be excited, which will enhance the magnetic energy releasing rate and scatter the energetic particles accelerated by the induced super electric field (Martens 1988; Litvinenko & Craig 2000; Craig & Litvinenko 2002; Litvinenko 2003).

* Supported by the National Natural Science Foundation of China.

More recent reconnecting experiment involving three-dimensional (3D) magnetic fields in the parameter regime of electron magnetohydrodynamics has been presented (Stenzel et al. 2003). The focus is on current-driven instabilities in the magnetic neutral sheet. Density fluctuations are observed in the neutral sheet and identified as current-driven ion sound turbulence. No lower hybrid turbulence or Buneman instabilities were detected. So, Stenzel et al. (2003) argued that only ion acoustic turbulence is excited in the magnetic reconnection, which enhances the resistivity and energy release rate. Therefore, ion acoustic instability should be considered in the particle acceleration in RCS.

As stated by Litvinenko (2003), since the magnitudes of the accelerating electric field and the turbulent analog of the Dreicer field are of the same order, the analytic solution of the distribution of the energetic particles is difficult to obtain when considering the effect of the turbulent wave. Hence, the existing results on particle acceleration inside the RCS were obtained without considering the effect of wave-particle interaction, and the predicted spectrum index of the energetic particles is about 1.5∼2.2, which is too hard to interpret the observations (Mori et al. 1998; Heerikhuisen et al. 2002; Miller et al. 1997; Aschwanden 2002).

In principle, when the proper Fokker-Planck equation including the terms of the time-dependent electromagnetic field and the ion acoustic turbulence is self-consistently solved, the spatial dependence of the electron distribution could be obtained. However, it is very difficult to bring this about. Since the Lorentz force cannot change the kinetic energy but only changes the orbit of the particles, we try to approach the evolution of energetic particles in two-steps. In the first step, through solving the movement equation for a single electron in a turbulent RCS, we check the effect of the Lorentz force on the electron motion and deduce the timescales of the electron acceleration inside the current sheet in different positions. In the second step, we investigate the time-dependent distribution of the non-thermal electrons by solving the Fokker-Planck (hereafter FP) equation and calculate the spectrum with the electron acceleration timescales and compare them with the observed hard X-ray emissions in the impulsive phase of flares. This paper is outlined as follows. In Section 2, ion-acoustic instability and the anomalous resistivity are reviewed. The electron acceleration timescales are studied in Section 3. In Section 4, the calculated electron spectra and a comparison with observation are given. In Section 5, a discussion and conclusions are presented.

2 ION ACOUSTIC INSTABILITY AND THE ANOMALOUS RESISTIVITY

In the limit of ignorable turbulence in the sheet with a single particle model, Speiser (1965) first found that after the electrons and protons are ejected out of the current sheet, they all have almost the same velocity along the magnetic field lines, $V_{\rm beam} = 2Ec/B_\perp$, in the two dimensional magnetic field structure, where E is the induced electric field strength, c is the speed of light in vacuum, $B_\perp$ is the component of the magnetic field perpendicular to the sheet plane that leads the electrons out of the sheet without being further accelerated. The averaged velocity of the particles inside the sheet is about half of the beam velocity $V_{\rm beam}$ (Martens & Young 1990). In the case of 3D magnetic field structure ($\boldsymbol{B} = (-y/aB_0, B_\perp, B_\parallel)$), Litvinenko (1996) found that $B_\parallel$ keeps the electrons inside the sheet to be accelerated, here $B_\parallel$ is the component of the magnetic field parallel to the sheet plane and along the electric field. He argued that the maximum energy and the acceleration time are limited. With the typical values of $B_0 = 100\,\mathrm{G}$, $B_\perp = 1\,\mathrm{G}$, $B_\parallel = 100\,\mathrm{G}$, the induced electric field $E_0 = 10V\,\mathrm{cm}^{-1}$ and the sheet half thickness $a = 10^2\,\mathrm{cm}$, Litvinenko (1996) figured out that the acceleration time is about $10^{-6}\,\mathrm{s}$ and the maximum energy is about 100 keV for the electrons. In addition, near the X-type neutral point

where $B_\perp$ becomes very small, Litvinenko (2000) deduced that the electron acceleration time is about 3×10^{-4} s and the maximum energy is about 30 MeV .

Since the timescale for the current sheet reconnection may be estimated to be the same order as the rise time for the hard X-ray emissions, it is about tens of seconds or minutes, while the growth time of the ion acoustic wave is $(m_i/m_e)^{1/2}\omega_{pi}^{-1}$ of $(0.3 \sim 1) \times 10^{-7}$ s with plasma density $10^8 - 10^9$ cm^{-3} (Spicer 1981, here ω_{pi} the ion plasma frequency). Moreover, the electrons and protons inside the sheet are accelerated in opposite directions with a velocity much larger than the electron thermal velocity v_e (Martens 1988; Martens & Young 1990). All of these show that the ion-acoustic instability should be excited.

With the two one-dimensional drift Maxwellian distributions respectively for the electrons and ions, the critical drift velocity for the onset of ion acoustic instability depends on the ratio of the electron temperature T_e to the ion temperature T_i (fig.1 of Smith & Priest 1972). Due to the ion Landau damping, which tends to cancel the wave growth rate due to the electron inverse Landau damping, the drift velocity increases with the ratio of T_e/T_i. When $T_e = T_i$, the required drift velocity is of the order of the electron thermal velocity (Smith & Priest 1972; de Kluiver et al. 1991). Therefore, the ion-sound instability may be easily excited in the RCS, and the plasma in the RCS should be in the turbulent state (Martens 1988; Litvinenko 2003).

Because the ion-acoustic waves are much more effective in deflecting the particles through some angle than in accelerating them along the direction of the velocity, they are responsible for plasma heating rather than particle acceleration (Smith & Priest 1972; Takakura 1988). Furthermore, the occurrence of the ion acoustic wave depends on the collective behavior of electrons and ions inside the sheet. So, the electrons in the RCS are accelerated by the induced super Dreicer field and also scattered by the turbulent ion-acoustic wave, no matter how long an electron dwells inside the current sheet.

The anomalous electric conductivity of a plasma with developed ion acoustic turbulence for the local electric field $E \gg E_D$ with $T_e = T_i$ (eq.(2.148) of Bychenkov et al. (1988) and references therein) is:

$$\sigma_A \simeq 0.4\omega_{pe}\left(\frac{8\pi n_e \kappa T_e}{E^2}\right)^{1/4}, \tag{1}$$

where ω_{pe} is the electron plasma frequency, $E_D = m_e v_e/e\tau_s$ is the Dreicer field and τ_s the electron and ion collision time with $\tau_s = m_e^2 v_e^3/(4\pi n_e e^4 \ln\Lambda)$, v_e the electron thermal velocity and $\ln\Lambda$ the Coulomb logarithm.

For the relationship between the effective collision frequency $\nu_{\rm eff}$ for thermal electrons and the effective conductivity $\sigma_A = e^2 n_e/m_c\nu_{\rm eff}$, we have from Eq.(1),

$$\nu_{\rm eff} = 2.67 \times 10^6 E^{1/2} n_e^{1/4} T_e^{-1/4}. \tag{2}$$

Substituting the typical values of the plasma density of 10^8 cm^{-3}, of the temperature of 10^6 K and of the induced electric field strength of $1 \sim 10$ V cm^{-1} into Eqs.(1)$\sim$(2), we have an effective collision frequency $\nu_{\rm eff}$ of $(0.844 \sim 2.67) \times 10^7$ s^{-1}. This suggests that in the turbulent RCS, wave-particle interaction should be considered on the acceleration timescales of $10^{-6} \sim 10^{-5}$ s.

In addition, if we assume that the enhanced conductivity mainly results from the occurrence of the ion acoustic instability, the ratio ξ of the ion-acoustic wave energy density to thermal energy density may be expressed in terms of the effective collision frequency:

$$\xi = \nu_{\rm eff}/\omega_{pe} = 0.474 \times 10^2 E^{\frac{1}{2}}(\text{V cm}^{-1}) T_e^{-\frac{1}{4}}(\text{K}) n_e^{-\frac{1}{4}}(\text{cm}^{-3}). \tag{3}$$

The previous results on the particle's orbit in the RCS did not take turbulence in to account, so, in the next section, we will consider the wave-particle interaction and deduce the timescale of the electron acceleration in the turbulent RCS by numerically solving equation of motion of a single particle.

3 ACCELERATION TIMESCALES OF ELECTRONS IN TURBULENT RCS

Considering the effect of turbulence on electron acceleration, the relativistic equation of motion for an electron of mass m_e and charge e is:

$$\frac{d}{dt}\frac{\boldsymbol{u}}{\sqrt{1-\frac{u^2}{c^2}}} = \frac{q}{m_e}(\boldsymbol{E}+\frac{1}{c}\boldsymbol{u}\times\boldsymbol{B}) - \frac{\nu^*_{\rm eff}\boldsymbol{u}}{\sqrt{1-\frac{u^2}{c^2}}}\,. \tag{4}$$

The 3D electromagnetic field form is (Litvinenko 1996):

$$\boldsymbol{B} = (-y/aB_0, B_\perp, B_\parallel), \qquad \boldsymbol{E} = (0,0,E)\,, \tag{5}$$

where E and $B_\parallel$ can be assumed to be constants. In order to accelerate the electrons sufficiently to produce hard X-ray emission in solar flares, a large component of parallel magnetic field is needed (Litvinenko 1996).

Like Coulomb collisions, the collision frequency due to ion-acoustic wave scales as Equation(6) for $u < v_e$ and Eq. (7) for $u > v_e$ (Spicer 1981):

$$\nu^*_{\rm eff} = \nu_{\rm eff}\frac{u}{v_e}, \tag{6}$$

$$\nu^*_{\rm eff} = \nu_{\rm eff}\frac{v_e^3}{u^3}. \tag{7}$$

As the particles always drift into the neutral sheet at velocity $\boldsymbol{E}\times\boldsymbol{B}_x$ and are accelerated mainly there (Litvinenko 1996; Heerikhuisen et al. 2002), we take the initial coordinates $y_0 = 0, z_0 = 0$. Assuming $B_\perp = 5x$(G) with x in units of half sheet width b, $B_0 = B_\parallel = 100\,$G, we integrate the particle trajectories at time steps of $10^{-14}\,$s with the forth-order Runge-Kutta method and stop the calculations when the electron is ejected out of the sheet. The final energy and acceleration time may be obtained for different initial velocities and positions along the x axis.

In addition, Litvinenko (1996) deduced the analytical expressions for the final energy and acceleration time when $B_\parallel > (\frac{mc^2EB_0}{eaB_\perp})^{\frac{1}{2}}$ and when turbulence is ignored,

$$\varepsilon = \frac{B_\parallel}{B_\perp}eEa\ , \qquad t = \Big(\frac{B_\parallel}{B_\perp}\frac{2am}{eE}\Big)^{\frac{1}{2}}. \tag{8}$$

For an electric field strength E of 5V cm^{-1}, a plasma density n_e of 10^8 cm^{-3}, a temperature T_e of 10^6 K, the analytical and numerical results with and without the term of turbulence are given in Figure 1. The acceleration time versus the initial position for different electric field strengths is shown in Figure 2, the other parameters being the same as in Figure 1.

It is shown by Fig.1 and our calculations that: (1) Because of the wave-particle scattering effect, the final energy decreases and the accelerating time increases with increasing turbulence in the region $0.3 \le x \le 1.0$, while in the region $0.0 \le x \le 0.3$, the effect of wave particle scattering is not apparent for the case where that the accelerated electron velocity is much larger than the thermal velocity. (2) Since the displacement of the electron is small along the

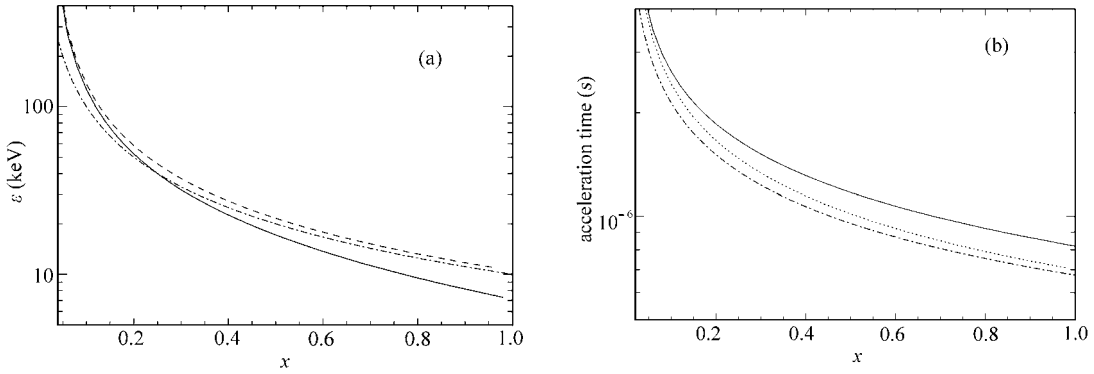

Fig. 1 Initial position versus the final energy (a) and the acceleration time (b). Solid lines with turbulence; dash lines, no turbulence; dash-dotted line for the analytic results without turbulence.

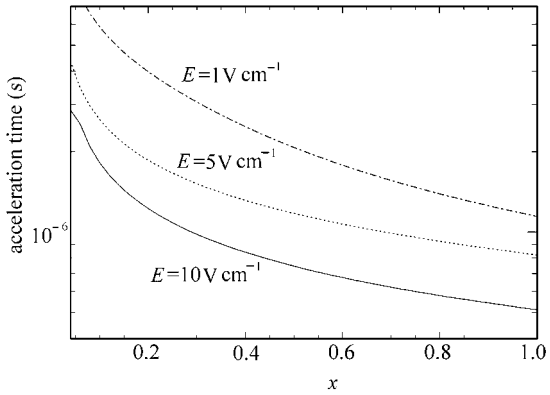

Fig. 2 Acceleration time versus initial position for different induced electric field strengths.

x-axis and the transverse component of magnetic field varies slowly, we may ignore its variation over the particle's orbit and take the acceleration time to be a function of the initial position. (3) The electron may be accelerated only when the initial velocity is larger than a critical value of about $1.2v_e$.

4 CALCULATION OF THE ELECTRON SPECTRA AND COMPARISON WITH OBSERVATION

In principle, the energetic electron spectrum may be inferred by solving the FP equation including the terms of the electromagnetic field and the ion acoustic turbulence. Because the Lorentz force changes only the orbit of the electrons without increasing their kinetic energy, the effect of the magnetic field is involved on the timescales stated above. The space dependence can also be

simplified bcause the change in the transverse component of the magnetic field over the electron orbit can be ignored. Therefore, using the acceleration timescales of the RCS electrons worked out in Section 3, the final spectrum may be deduced from the solution of the FP equation that includes the induced electric field and the ion acoustic turbulence.

4.1 Basic Equations

When the ion-acoustic turbulence is taken into account, the evolution of the energetic electrons accelerated by the electric field can be obtained from the following FP equation (Wiley et al. 1980; Takakura 1988; Wu et al. 2001; Gan & Wang 2002):

$$\frac{\partial f}{\partial t} + q\boldsymbol{E}\cdot\frac{\partial f}{\partial \boldsymbol{P}} = \left(\frac{\partial f}{\partial t}\right)_{IS}. \tag{9}$$

Considering nonlinear Landau damping on ions, Kadomtsev (1965) first derived the spectrum of ion-sound waves that was consistent with some experimental results. Then, Takakura (1988) derived the expression for the scattering of the ion-sound turbulence on electron acceleration in the case of an isotropic distribution of waves,

$$\left(\frac{\partial f}{\partial t}\right)_{IS} = \xi f_p\Big\{1.2\frac{m_e}{m_i}\frac{P_T^5}{P^2}\frac{\partial}{\partial P}\left(\frac{R_2 f}{P^2}\right) + 6.1R_1\frac{P_T^3}{P^3}\frac{\partial(1-\mu^2)\partial f}{\partial\mu^2}\Big\}. \tag{10}$$

In Eq. (10), R_1, R_2 are the relativistic correction factors, $R_1 = (1-v^2/c^2)^{-1/2}, R_2 = R_1^3$, and $v_e = \sqrt{kT_e/m_e}$, $P_T = m_e v_e$, and $f_p = 8.98\times10^3\sqrt{n_e}$ Hz is the electron plasma frequency.

From Eqs.(9) and (10) with $\boldsymbol{E} \parallel \boldsymbol{z}$, pinch-angle cosine $\mu = \hat{p}\cdot\hat{z}$, we obtain, in terms of the dimensionless variables $\tau = t/\tau_s, p = P/P_T$ and $\epsilon = E/E_D$,

$$\frac{\partial f}{\partial \tau} = -\epsilon\Big\{\frac{\mu}{p^2}\frac{\partial(p^2 f)}{\partial p} + \frac{1}{p}\frac{\partial}{\partial\mu}(1-\mu^2)f\Big\}+$$

$$\xi f_p\tau_s\Big\{1.2\Big(\frac{m_e}{m_i}\Big)\frac{1}{p^2}\frac{\partial}{\partial p}\Big(\frac{R_2 f}{p^2}\Big) + 6.1R_1\frac{1}{p^3}\frac{\partial(1-\mu^2)\partial f}{\partial\mu^2}\Big\}. \tag{11}$$

Correspondingly, $R_1 = (1+\alpha p^2)$, $\alpha = v_T^2/c^2$. The initial distribution function is set like a Maxwellian drift along the $+\boldsymbol{z}$ direction,

$$f(p,\mu) = \frac{n_0}{(\sqrt{\pi}P_T)^3}\exp\Big\{-\frac{P^2+P_j^2-2PP_j\mu}{P_T^2}\Big\} =$$

$$\frac{n_0}{(\sqrt{\pi}P_T)^3}\exp(-p^2-p_j^2+2pp_j\mu), \tag{12}$$

where $P_j = m_e V_d$ is the initial displacement momentum, $p_j = P_j/P_T$. Since the bulk electrons in RCS are accelerated by super Dreicer electric field, the initial value of p_j is assumed to be 1. Numerically solving Eq. (11) and integrating over the angle, we have:

$$f(p,t) = \int_{-1}^{1} 2\pi p^2 f(p,\mu,t)d\mu. \tag{13}$$

Since the electron energy ε corresponding to momentum p is $\varepsilon = (R_1-1)m_e c^2$, the time-dependent distribution of the electrons with energy ε can be expressed as:

$$f(\varepsilon,t) = f(p,t)\frac{\partial p}{\partial\varepsilon} = f(p,t)\frac{R_1}{\alpha p m_e c^2}. \tag{14}$$

The energetic electron spectrum may be estimated from the continuity equation and the acceleration timescales,

$$\frac{dN(\varepsilon,t)}{d\varepsilon} \sim \int f(x,\varepsilon,t)dx. \tag{15}$$

Now, we use the explicit difference scheme to solve Eq.(11), together with the powerful method of operator splitting, which is a common method for numerically solving multidimensional differential equations (Hamilton & Petrosian 1992; Smith & Miller 1995; Park & Petrosian 1996). First, the upwind form is used to determine the finite difference operators for the momentum term accurate to the first-order in time and momentum. Secondly, the Lax-Wendroff scheme is used to determine the pinch-angle diffusion term, to the same accuracy, in time and pinch-angle cosine. The time, momentum and pinch-angle cosine steps are respectively 2×10^{-11} s, $3P_T$ and 0.125, which are chosen to ensure stable solutions. The same results are obtained if these steps are divided by two. Because only the electrons in the runaway regime ($u > 1.2v_e$) can be accelerated, the number of electrons in the runaway regime is conserved.

4.2 The Evolution of Accelerated Electrons and Their Spectrum

It is widely accepted that the hard X-ray and continuous γ-ray emissions in the impulsive phase of flares result from the bremsstrahlung of all energetic electrons which may be accelerated by a DC electric field inside the RCS. In the 3D magnetic field, the electrons may be ejected out of the RCS before they have acquired the maximum energy. Hence, it is necessary to provide time-dependant distribution of the energetic electrons for different parameters.

For typical values of the temperature T_e of 10^6 K and the plasma density n_e of $10^8\,\mathrm{cm}^{-3}$ in RCS, we obtain the evolution of $f(\varepsilon,t)$ for different electric field intensities E of $1 \sim 10\,\mathrm{V\ cm}^{-1}$ (Fig. 3). The corresponding ratio of the ion-acoustic wave energy density to thermal energy density is estimated by Eq. (3).

It is well known that the induced electric field strength E depends on both the inflow velocity V_{in} and the magnetic field strength B near the RCS, and so varies during the impulsive phase of flares. The observation and numerical simulation showed that the electric field strength E is about a few V cm^{-1} (Foukal & Behr 1995; Lin & Forbes 2000). From Fig. 3, it is suggested that the different values of E generate the different distributions of electrons and the diversity of hard X-ray spectrum.

Integrating the distribution function along the x-axis (Eq. (15)) with different acceleration times in the different positions (Fig. 2), we obtain the non-thermal electron spectrum for different electric field strengths (Fig. 4a), different temperatures (Fig. 4b) and different plasma densities (Fig.4c), the other parameters being held the same as in Fig. 3(a).

It is shown in Fig. 4a that, when the electric field strength changes from $1\,\mathrm{V\ cm}^{-1}$ to $10\,\mathrm{V\ cm}^{-1}$, the energetic electron spectrum may be fitted with a power-law over the range $20 \sim 100\,\mathrm{keV}$, with index $3 \sim 10$. If $B_\perp$ is not small enough, the acceleration time becomes small and the energetic electron spectrum becomes soft. For example, if the acceleration time is less than 10^{-6} s, the spectral index is about 6 from Fig. 3b.

Up to now, recognized evolution of hard X-ray emissions has been classified into three types (A, B and C, Tanaka 1987). For type B (impulsive) and type C (gradual-hard), the hard X-ray emission can be expressed as a power-law in the energy range ($20 \sim 100$ keV), and the spectral index is respectively about $3.5 \sim 6$ and $2.5 \sim 4$. The corresponding spectral index of the energetic electrons is about $3.5 \sim 7$ in a thick target model (Brown 1971; Hudson et al. 1978). Type A is the thermal one.

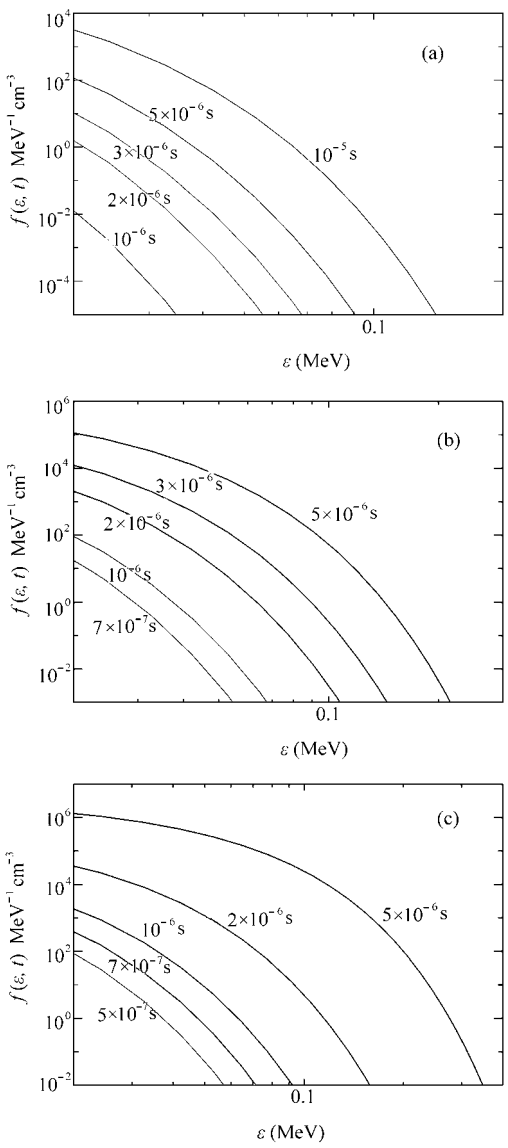

Fig. 3 Evolution of the accelerated electrons for different electric field strengths and for $n_e = 10^8\,\mathrm{cm}^{-3}$ and $T_e = 10^6\,\mathrm{K}$: (a) E=1 V cm^{-1}; (b) E=5V cm^{-1}; (c) E=10 V cm^{-1}.

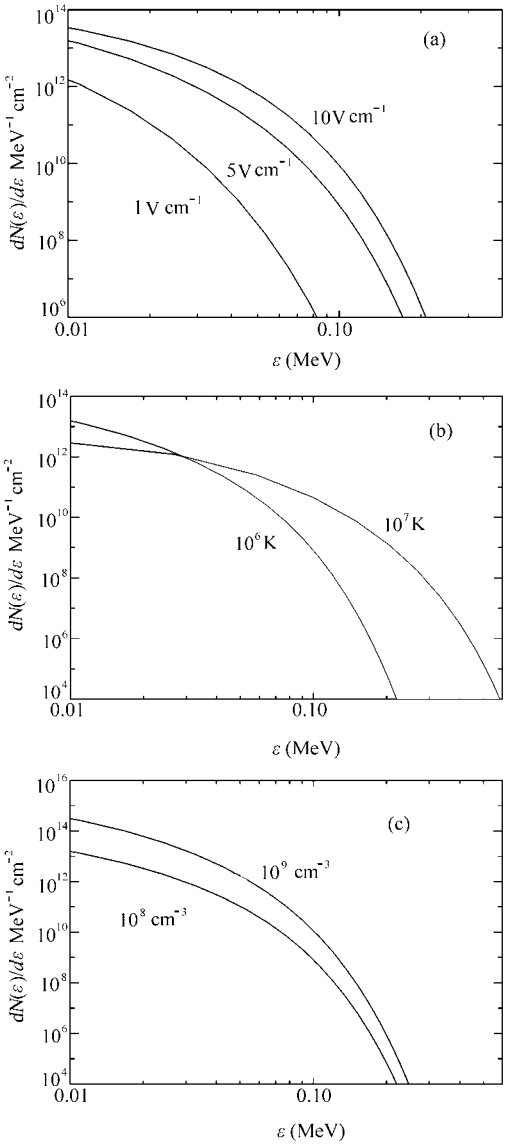

Fig. 4 Energy spectrum of the accelerated electrons for different parameter values: (a) $E = 1 \sim 10\,\mathrm{V\ cm}^{-1}$, $n_e = 10^8\,\mathrm{cm}^{-3}$, $T_e = 10^6\,\mathrm{K}$; (b) $E = 5\,\mathrm{V\ cm}^{-1}$, $n_e = 10^8\,\mathrm{cm}^{-3}$, $T_e = 10^6 \sim 10^7\mathrm{K}$; (c) $E = 5\mathrm{V\ cm}^{-1}$, $n_e = 10^8 \sim 10^9\,\mathrm{cm}^{-3}$, $T_e = 10^6\,\mathrm{K}$.

The above calculations suggest that when considering the ion-acoustic wave-particle scattering in the electron acceleration inside the RCS, the evolutionary property of the hard X-ray spectrum can be interpreted by plausible parameters and magnetic structure. In addition, from Fig. 4b and Fig. 4c we see that the plasma density and temperature have little effects on the evolution of the energetic electrons except in the high energy tail in Fig. 4b.

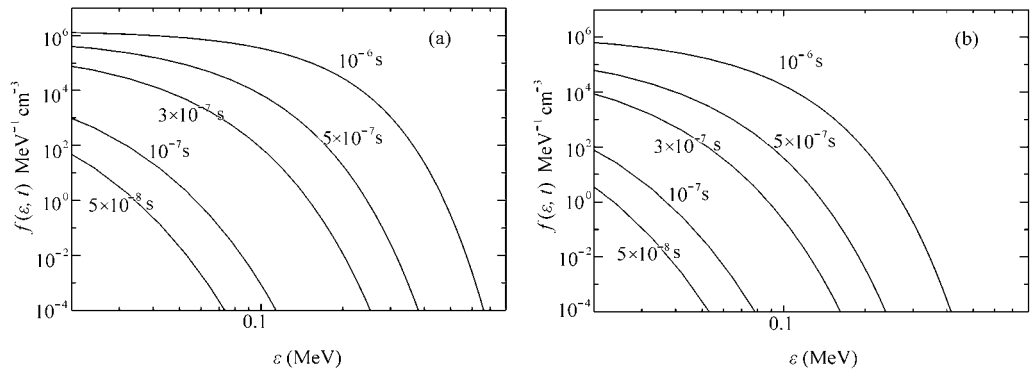

Fig. 5 Evolution of the accelerated electrons with the electric field strength (a) E=90 V cm^{-1}; (b) E=50 V cm^{-1}

4.3 Analysis of electron acceleration in the 2000 March 16 C9.0 flare

Using the time profiles of Yohkoh hard X-ray and OVSA microwave emissions, BBSO H_α images and magnetograms, Qiu et al. (2002) studied the evolution of the electric field and its relationship to the hard X-ray and microwave emissions in the 2000 March 16 C9.0 flare. They inferred that during the major impulsive phase from 18:35:40 to 18:35:50 UT, the electric field was as high as 90 V cm^{-1}, the flux of energetic electrons was about 10^{34} in the energy range of 20–85 keV with a power-law index of 3–5, and about 10^{30} above 100 keV with a power-law index of 1.5–3. They thought that the former was accelerated by DC electric field, while the latter was accelerated by some other mechanism.

According to the properties of particle acceleration in RCS, we argue that these energetic electrons may be accelerated by the same electric field with a different effective acceleration time. The following calculations (Fig. 5) show that this may be true. The energetic electrons in the range $20 \sim 80$ keV were mainly accelerated during $10^{-8} \sim 10^{-7}$ s in a relatively strong vertical magnetic field to a power-law with index about 3–5. The energetic electrons in the above 100 keV were mainly accelerated after 10^{-7} s in a relatively weak vertical magnetic field to a power-law with index about 1.5–3.

5 DISCUSSION AND CONCLUSIONS

Fast magnetic reconnection is recognized as the most efficient way for the non-potential magnetic energy release and the primary particle acceleration in a solar flare. Due to the complexity of the reconnection, though many studies have been carried out, there is still no self-consistent solution that includes the evolution of the time-dependent electromagnetic field and the particle acceleration in the driven RCS. The present theory for particle acceleration has not taken the wave-particle interaction into account. So, the predicted energetic particle spectrum is too hard to be consistent with the observations.

Because the drift velocity of the electrons is much larger than the threshold for the occurrence of ion acoustic wave in RCS, we assume that the ion-acoustic wave was excited. Of course, some other waves may also be excited to enhance the reconnection rate (for example, whistler waves (Deng & Matsumoto 2001)). More refined treatments are required to identify which wave

will be first excited and have more effect on particle acceleration using particle simulation in fast driven RCS with time-dependent electromagnetic field that includes the background field and the spontaneous field due to the particle motion.

Considering that the effective acceleration time is limited in a 3D magnetic structure, we approach the time-dependent particle distribution in two steps. First, the equation of motion of the electron is solved and the acceleration timescales are obtained for different parameter values. Then, the FP equation that includes the terms of electric field and ion-acoustic turbulence scattering, is numerically worked out. It should be pointed out that the influence of ion-sound waves on the electron motion and acceleration is checked under the assumption of isotropic distribution of waves without considering the effect of the magnetic field. So, it is valid only along the magnetic field and only approximately so across the magnetic field. Though we did not solve the entire FP equation that includes the terms of the time-dependent electromagnetic field and the ion acoustic turbulence, self-consistently in one step, the results are still meaningful. Our solution shows that the electric field strength and the acceleration time do take more important roles on the final energetic particle distribution. With plausible parameter values, we can interpret the observed properties of the hard X-ray spectra.

In order to seek more observational evidence for this model, simultaneous multi-wavelength observations for the same event should be carefully analyzed, including the magnetic field, H_α, microwave type III bursts, hard X-ray and γ-ray as well as microwave emissions. From these, we may infer the time profile of the induced electric field and accelerated energetic electrons. It is important for us to construct a plausible physical model and correctly understand the acceleration mechanism in RCS.

In summary, our conclusions can be stated as follows:

(1) Scattering of energetic electrons by ion-acoustic turbulence should be considered in the process of electron acceleration inside the RCS. For typical RCS parameters, the accelerated electrons may have an approximately power-law distribution in the energy range $20 \sim 100\,\mathrm{keV}$ and a spectral index in the range $3 \sim 10$.

(2) Different active regions may have different evolutionary characteristics that generate induced electric fields of different durations and strengths, and hence different acceleration times. This is an important factor for the diversity of the photon spectrum that may be used to account for the observed hard X-ray and γ-ray emissions.

Acknowledgements The authors are very grateful to the referee for his(her) valuable comments and suggestions. We are also grateful to Prof. Wang D. Y. for helpful discussions. This work is supported by the National Natural Science Foundation of China (No.10333030 and 10273025).

References

Aschwanden M. J., 2002, Space Science Review, 101, 1
Brown J. C., 1971, Solar Phys., 18, 489
Bychenkov V. Yu., Silin V. P., Uryupin S. A., 1988, Physics Rep., 164, 119
Craig I. J. D., Litvinenko Y. E., 2002, ApJ, 570, 387
de Kluiver H., Perepelkin N. F., Hirose A., 1991, Physics Rep., 199, 281
Deng X. H., Matsumoto H., 2001, Nature, 410, 557
Foukal P. V., Behr B. B., 1995, Solar Phys., 156, 293
Gan W. Q., Wang D. Y., 2002, The Physics of Solar High energy, 1st ed., Science Press

Hamilton R. J., Petrosian V., 1992, ApJ, 398, 350
Heerikhuisen J., Litvinenko Y. E., Craig I. J. D., 2002, ApJ, 566, 512
Hudson H. S., Canfield R. C., Kane S. R., 1978, Solar Phys., 60, 137
Kadomtsev B. B., 1965, Plasma Turbulence, New York: Academic Press
Lin J., Forbes T. G., 2000, J. Geophys. Res., 105, 2375
Litvinenko Y. E., 1996, ApJ, 462, 997
Litvinenko Y. E., Craig I. J. D., 2000, ApJ, 544, 1101
Litvinenko Y. E., 2000, Solar Phys., 194, 327
Litvinenko Y. E., 2003, Solar Phys., 212, 379
Martens P. C. H., 1988, ApJ, 330, L131
Martens P. C. H., Kuin N. P. U., 1989, Solar Phys., 122, 263
Martens P. C. H., Young A., 1990, ApJS, 73, 333
Masuda S., Kosugi T., Hara H. et al., 1994, Nature, 371, 495
Miller J. A., Cargill P. J., Emslie A. G. et al., 1997, J. Geophys. Res., 102, 14659
Mori K., Sakai J., Zhao J., 1998, ApJ, 494, 430
Park B. T., Petrosian V., 1996, ApJS, 103, 256
Qiu J., Lee J., Gary D. E. et al., 2002, ApJ, 565, 1335
Smith D. F., Priest E. R., 1972, ApJ, 176, 478
Smith D. F., Miller J. A., 1995, ApJ, 446, 390
Somov B. V., Kosugi K., Hudson H. S. et al., 2002, ApJ, 579, 863
Speiser T. W., 1965, J.Geophys. Res., 70, 8211
Spicer D. S., 1981, Solar Phys., 70, 149
Stenzel R. L., Griskey M. C., Urrutia J. M. et al., 2003, Physics of Plasmas, 10, 2810
Takakura T., 1988, Solar Phys., 115, 149
Tanaka K., 1987, PASJ, 39, 1
Wiley J. C., Choi D. I., Horton W., 1980, Phys. Fluids, 23, 2193
Wu G. P., Xu A. A., 1996, Chinese J. Sp. Sci., 16, 56
Wu G. P., Xu,A. A., Tang Y. H., 2001, Chin. Astron. Astrophys., 25, 221
Yokoyama T., Akita K., Morimoto T. et al., 2001, ApJ, 546, L69